Supplementary Information (SI) for Journal of Materials Chemistry C.
This journal is © The Royal Society of Chemistry 2025

Assembly of van der Waals Structure from CVD-Grown 2-dimensional Materials Using Plasma-Treated Polyvinyl Chloride

Bin Xu[1,2#], Satoru Masubuchi[3#], Yusai Wakafuji[3], Yuanzhe Li[1], Tomoki Machida[3,*] ,Junichiro Shiomi[1,2,*]

[1]Department of Mechanical Engineering, The University of Tokyo, 7-3-1 Hongo, Bunkyo, Tokyo, 113-8656, Japan
[2]Institute of Engineering Innovation, The University of Tokyo, 2-11 Yayoi, Bunkyo, Tokyo 113-8656, Japan
[3]Institute of Industrial Science, The University of Tokyo, 4-6-1 Komaba, Meguro-ku, Tokyo 153-8505, Japan
[#]These authors contributed equally: Bin Xu, Satoru Masubuchi
[*] Corresponding author:
*tmachida@iis.u-tokyo.ac.jp (T. Machida)
[*]shiomi@photon.t.u-tokyo.ac.jp (J. Shiomi)

Methods

1. Fabrication of vdW stacking

Preparation of P-PVC stamp: To fabricate a P-PVC stamp for picking up CVD-grown 2D materials, a PVC stamp composed of a PVC film, PDMS dome, gel sheet, and slide glass was first fabricated. More details on the fabrication process are provided in previous studies[1,2]. A triple or single micro PDMS dome was fabricated on a glass slide to control the contact area between the stamp and 2D materials. A gel sheet (Gel-Pak, PF-20-X4) was attached to the sliding glass, and a PDMS droplet was deposited on the gel sheet and heated to form a PDMS dome. A commercially available PVC food wrap (Riken Technologies) was placed over the PDMS dome. The surface of the PVC/PDMS stamp was cleaned with isopropyl alcohol prior to use. The PVC stamp was then placed inside an ICP apparatus (Harrick Plasma, PDC-32G) and plasma-treated for 40 s. The plasma was generated using a radio-frequency power supply of 9 W after back pumping the chamber to a vacuum of approximately 280 Pa without adding any other gases. This pressure is a pivotal factor in reducing the amount of residual PVC, which was optimized as shown in Figure S9. The plasma pressure is critical as it determines the ion bombardment energy of the plasma, which can modify the molecular weight of the PVC during plasma treatment, thus influencing the glass transition, mechanical properties, solubility, and thermal stability. These properties are important for a successful transfer.

CVD synthesized WS2 and MoS2: In the CVD growth of WS_2, a three-zone tube furnace is utilized as the growth equipment. The precursor materials used are high-purity WO_3 (tungsten trioxide) and high-purity sulfur (S). The carrier gases employed are argon (Ar) at a flow rate of 200 sccm and hydrogen (H_2) at a flow rate of 20 sccm. During the process, the WO_3 is heated to 1000 ^oC, while the S is heated to 200 ^oC. A sapphire substrate was positioned 7 cm below the WO_3. The growth process is carried out for 10 minutes, resulting in the formation of WS_2 on the substrate.

In the growth of MoS_2, a dual-zone tube furnace with an 80mm diameter is used. Molybdenum trioxide (MoO_3) with a purity of 99.999% serves as the molybdenum source, while solid S of 99.999% purity is used as the sulfur source. Ar gas is employed as the carrier gas. During the growth process, the MoO_3 is heated to 650 ^oC, and the sulfur is heated to 180 ^oC. The growth is conducted under a pressure of 4000 Pa and lasts for 5 minutes. This process results in the formation of triangular MoS_2 crystals on a SiO_2/Si substrate.

Assembling vdW stacking from CVD-grown 2D materials using P-PVC stamp: Prior to transfer, the as-synthesized 2D materials were annealed at 300 °C for 1 h in an Argon-gas environment with 4% hydrogen. This stabilizes the adhesion between the substrate and 2D materials, prevents wrap-up, and cleans the top surface of the CVD-synthesized 2D materials by removing the adsorbed precursors. As a results, annealing can enhance the interlayer interactions for vdW stacking. Although annealing can enhance the adhesion between the substrate and 2D materials and cause the pick-up of the samples more difficult, this issue can be easily resolved using a P-PVC stamp and water-assisted pick-up method. The primary process of assembling a vdW heterostructure began with the selection of desired 2D crystals using an optical microscope. Subsequently, the desired 2D crystals were picked up by gently touching them with the stamp at approximately 50-70 ^oC and the chip surface was simultaneously injected with DI water. This

process was repeated to sequentially select the 2D materials and assemble the desired vdW stack on the P-PVC stamp surface. Finally, the resulting stack structure was transferred onto a targeted substrate at approximately 160 ^{o}C. During this step, the vdW stack and sacrificial layers were detached from the PVC and dropped onto the target substrate.

The cleaning process for removing the residual sacrifice layer: After the vdW stack structure was transferred onto the substrate, two steps were required to remove the sacrificial layer. The first step was to immerse the sample in a THF solution for 2 h, which dissolved most of the PVC sacrificial layer. The second step was to anneal the sample at 300 °C for 12 h in an environment of 4% hydrogen and 96% argon. This process removed the residual polymers from the sample top and enhanced interlayer vdW interactions[3].

2. Structure characterization of 2D materials

PL and Raman spectroscopy: We used Renishaw inVia with a wavelength of 532 nm to perform PL and Raman spectroscopic measurement. A grating of 600/mm and 3000/mm were used for the PL and Raman spectroscopic measurements, respectively. The peak positions were calibrated using a standard Si wafer by aligning the Si Raman peaks at 520.5 cm^{-1}.

3. Structure characterization of P-PVC stamp

FTIR: FTIR (Shimadzu, IRSpirit) was used to analyze the variation in the chemical components of the PVC film before and after the plasma and after annealing treatments. Specifically, we utilized the absorption mode and focused on the plasma-treated surface of P-PVC using an ATR unit. The ATR unit with a diamond prism and an incident angle of 30 °resulted in a penetration depth (d_p) of 814 nm for the PVC film, as calculated using the following equation.

$$d_p = \frac{\lambda}{2\pi n_1 \sqrt{\sin\theta^2 - (n_1/n_2)^2}},$$

Where λ is the wavelength of the incident light, n_1 and n_2 are the refractive index of the ATR crystal and sample, respectively, and θ is the incidence angle.

Liquid Chromatography: Liquid chromatography (Toso, HLC-8320GPC) was used to determine the molecular weight of the PVC films under diverse conditions. To prepare the sample, the PVC film was dissolved in THF (2 mg/mL). The measurement was conducted at 40 ^{o}C, with a flow rate of 0.6 mL/min, using a total of 20 μL of the solution. The measurements lasted for 15 min. The differential mobility of the PVC molecules inside the PTFE column depends on their molecular weights, allowing the individual components of PVC to be quantified based on the sequentially detected absorption signals at the column outlet. By analyzing these signals, the molecular weight of the PVC film was determined by fitting it onto a cubic curve. In addition to the four peaks corresponding to the PVC component, several downward peaks originating from THF were observed after 10 min.

DSC: A DSC (Netzsch, DSC 3500) was used to determine the glass transition temperature and melting point of the PVC films. In particular, we focused on the glass transition temperature, which is the temperature at which the PVC nanostructure becomes disordered, resulting in a sudden decrease in hardness. This transition is crucial because it affects the suitability of the soft stamp for picking up 2D materials. Additionally, we measured the melting point, which is vital for detaining 2D materials with a sacrificial layer because it causes the layer to melt and separate from the PVC, adhering to the substrate. Notably, we analyzed the entire PVC film, including both

the plasma-treated surface and the pristine sections that were not in contact with the reactive plasma.

DI-contact angle measurement: To examine the surface energy of the PVC surface, we used a home-made contact-angle measurement apparatus to measure the contact angle of DI water on the PVC film at room temperature (20 ^{o}C). Before measuring the contact angle, the PVC film was flattened, attached to a glass slide, and subjected to various treatments such as plasma treatment and annealing.

Figure

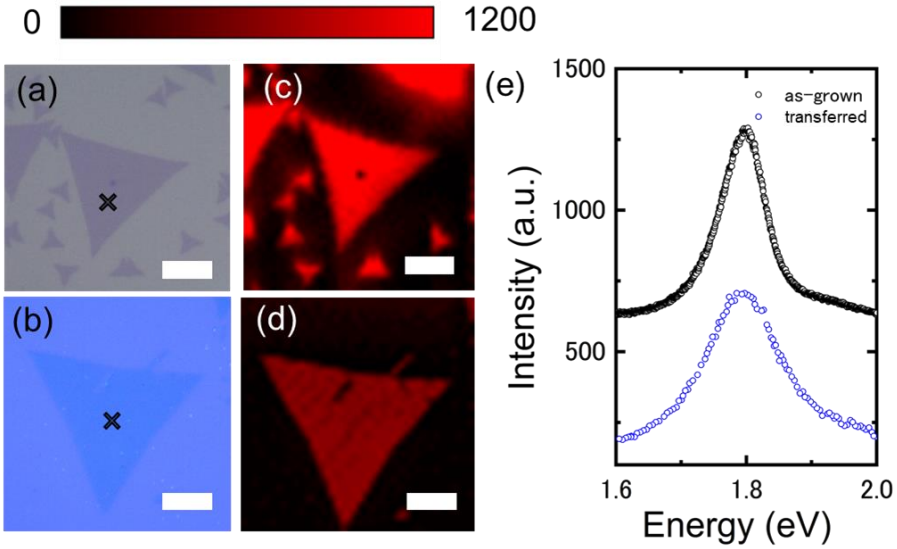

Fig. S1. The (a)(b)optical image, the (c)(d) PL intensity mapping and the (e) corresponding PL spectrum at the marked location of monolayer MoS_2 before (on SiO_2) and after transfer by P-PVC (on SiO_2), respectively. Scale bar is 20 μm.

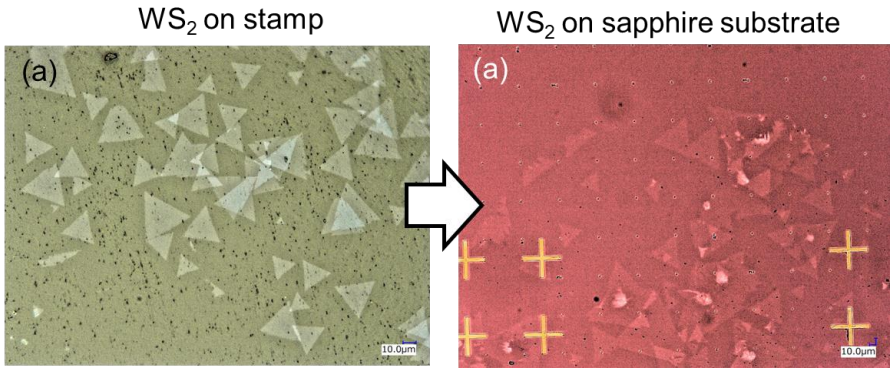

Fig. S2. (a) Pick up WS_2 in sequence and assemble the twist bilayer structure on the P-PVC stamp. (b) drop off the twist bilayer WS_2 on a sapphire substrate.

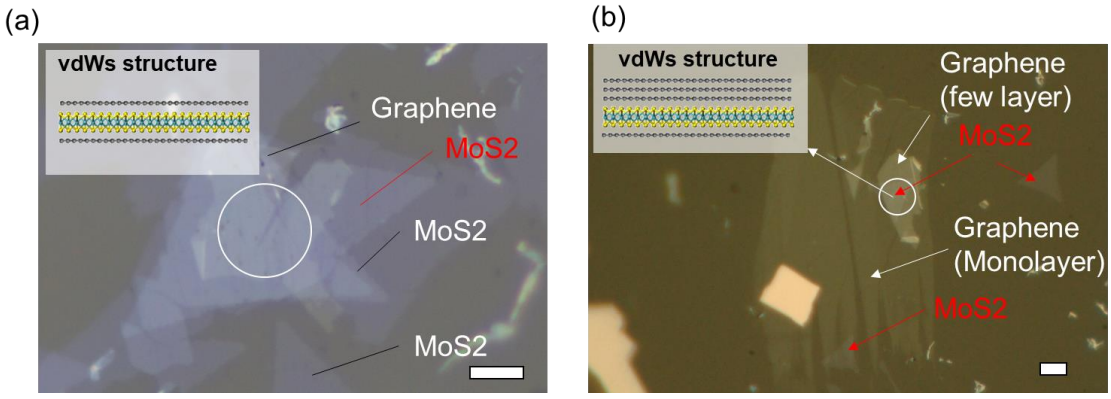

Fig. S3. assembly of vdWs using CVD synthesized MoS2 and mechanically exfoliated graphene. The structure of the vdWs stacking is shown in the inset. Scale bar is 30 μm.

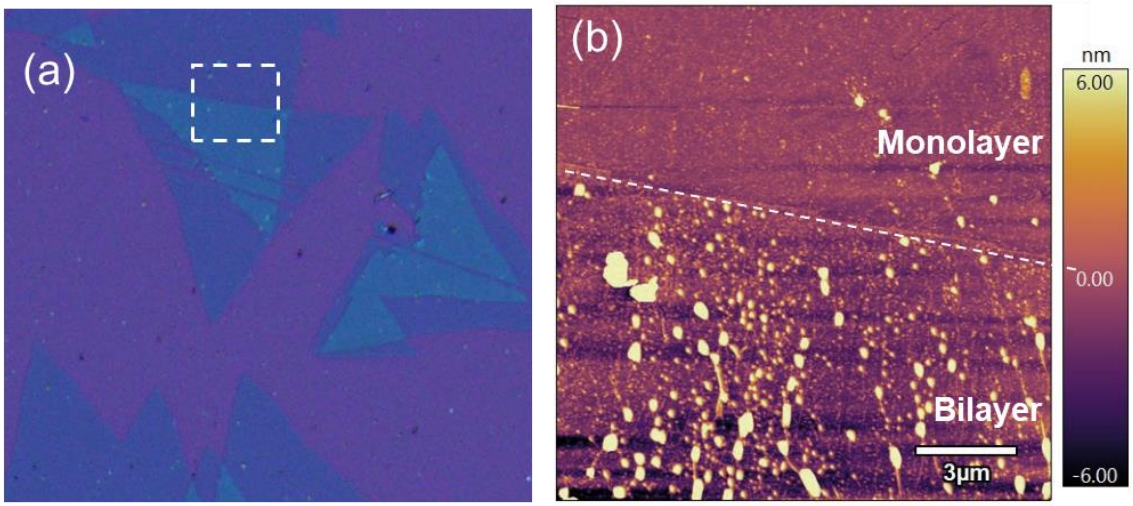

Fig. S4.(a) Optical and (b) AFM image of twsit bilayer WS_2 sample transferred on SiO_2 substrate. The dashed square in (a)(c) indicate the location of the AFM measurement. The monolayer region is clean, indicates little residual of PVC after transfer and cleaning, while some bubbles and wrikles appear at the bilayer region, which is strongly influenced by the the transfering circumstance and quality of 2D material.

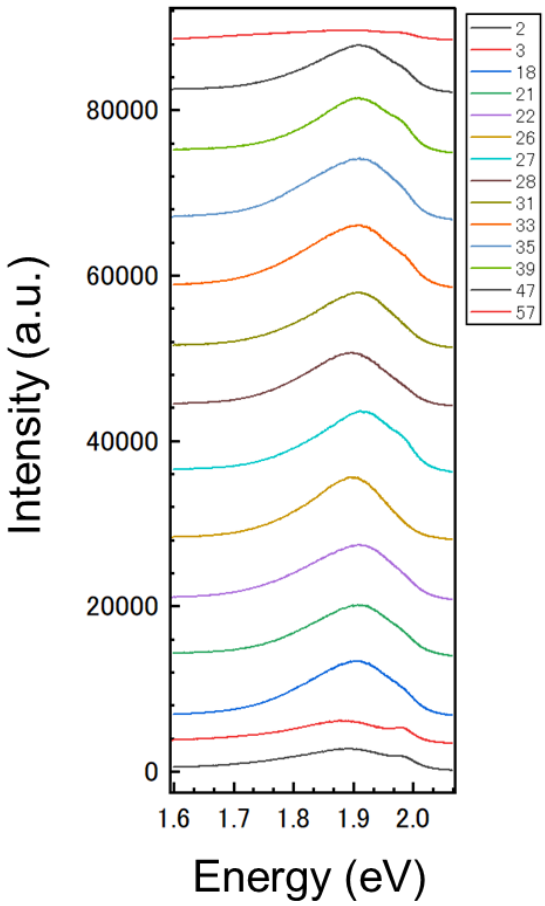

Fig. S5. PL spectrum of bilayer WS_2 with twist angel from 2 to 57 degrees.

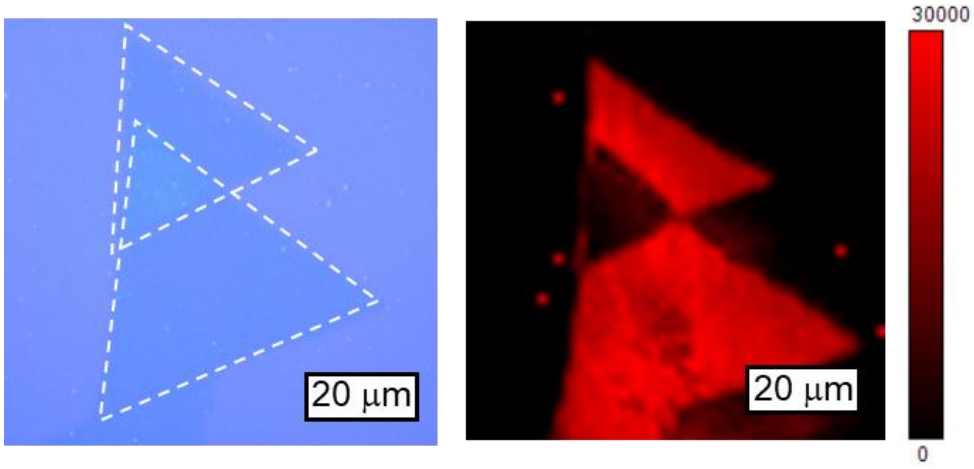

Fig. S6. PL intensity mapping of bilayer WS_2 with a twist angel of 57 degrees.

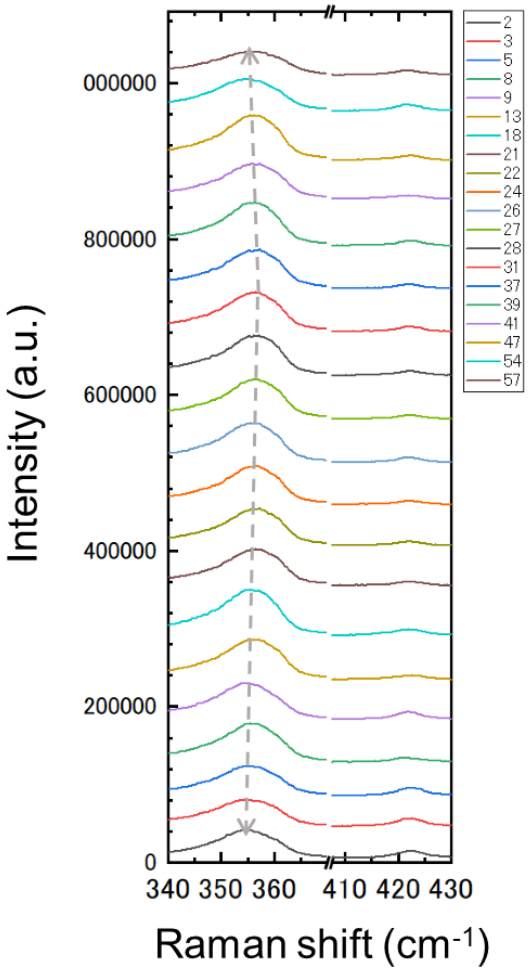

Fig. S7. Raman spectrum of bilayer WS_2 with twist angel from 2 to 57 degrees.

(a)

Temperature (°C)	50	60	70	80	90	100	110	120	130	140	150	160	170	180
PVC-exfolilated 2D materials														
PVC-CVD 2D materials_water														
P-PVC-CVD 2D materials_water														

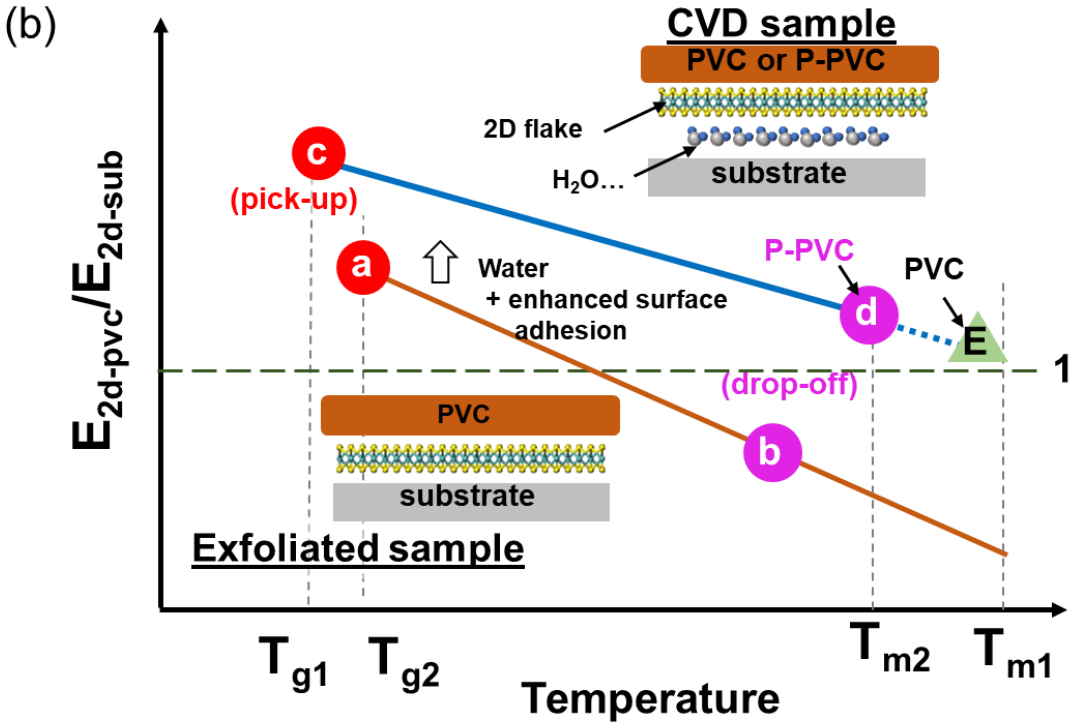

Fig. S8. (a) Temperature parameters of the transfer, including pick-up (red region) and drop-off (purple region), and the (b) corresponding expected adhesion variation between 2D materials /PVC stamp ($E_{2d\text{-}PVC}$), and between 2D materials/substrate ($E_{2d\text{-}sub}$) under various temperatures with two different experimental setups.

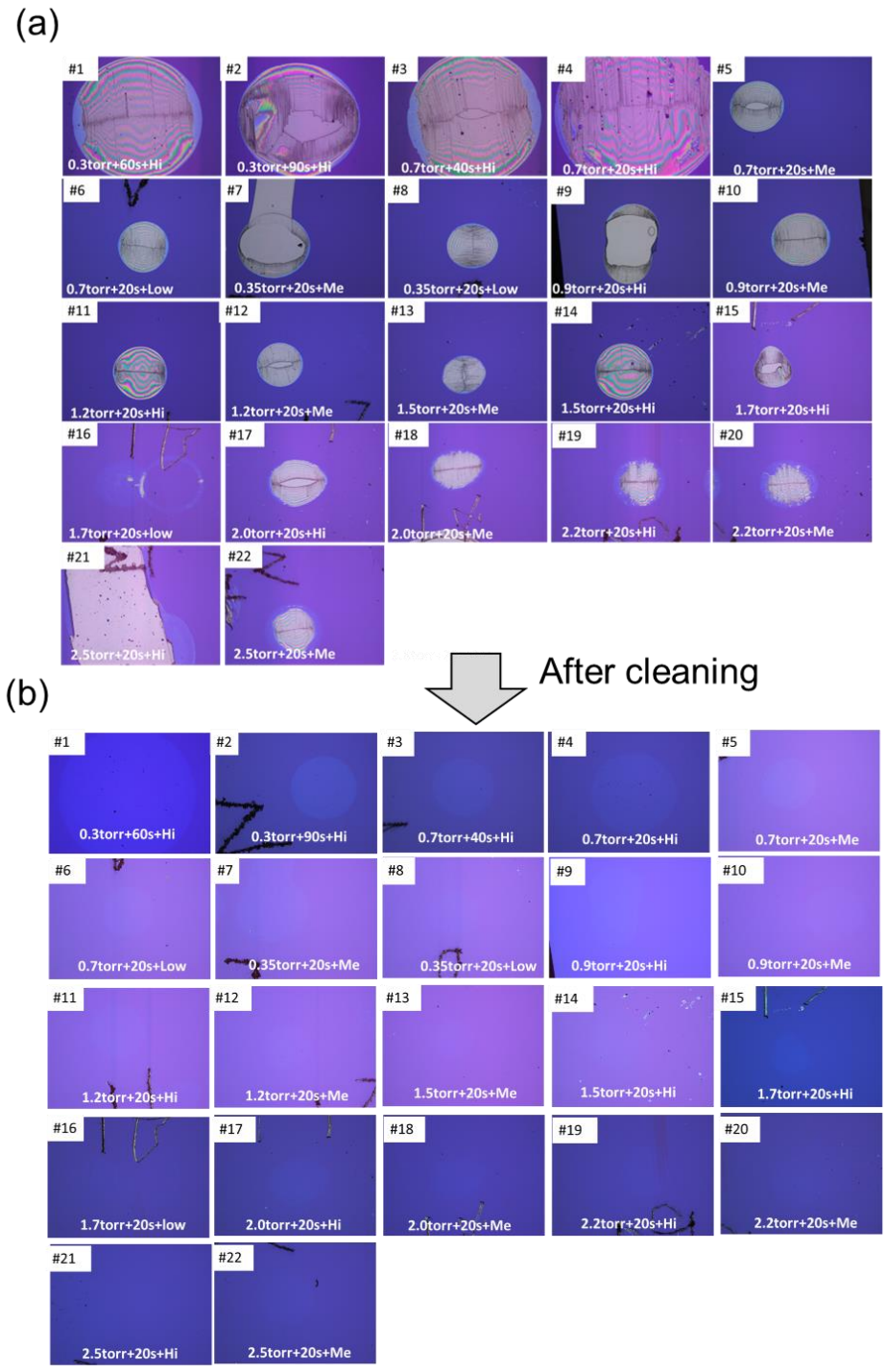

Fig. S9. the optical image of PVC residual (a) before and (b) after the cleaning with P-PVC treated under different plasma condition. (Low, Me, and Hi represent the plasma power, which is 6.8 W, 10.5 W, and 18 W, respectively)

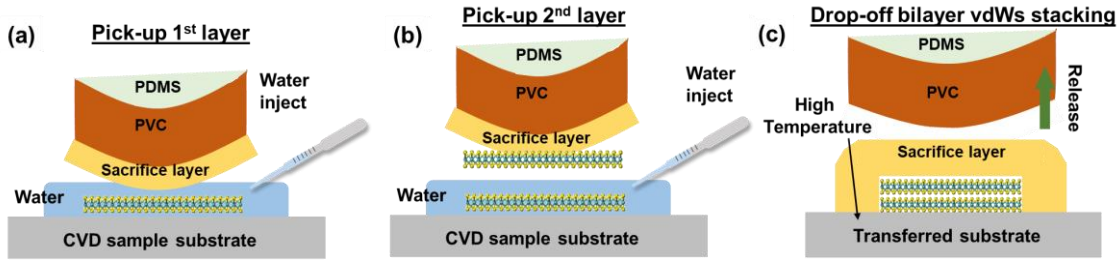

Figure S10. Schematic of the assembly of multi-layer vdW stacking using P-PVC.

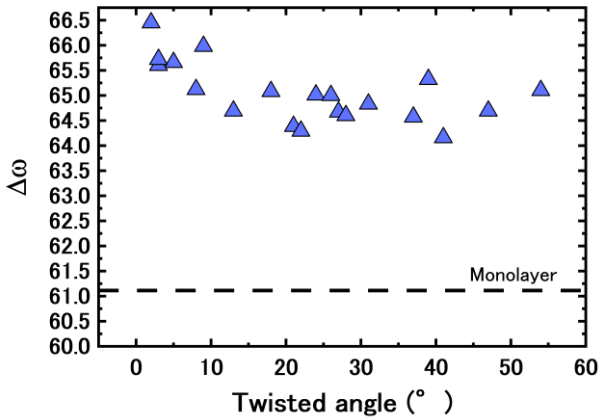

Figure S11. Distance in between (Δω) A1g and E2g modes in monolayer and bilayer WS_2 with different twist angles.

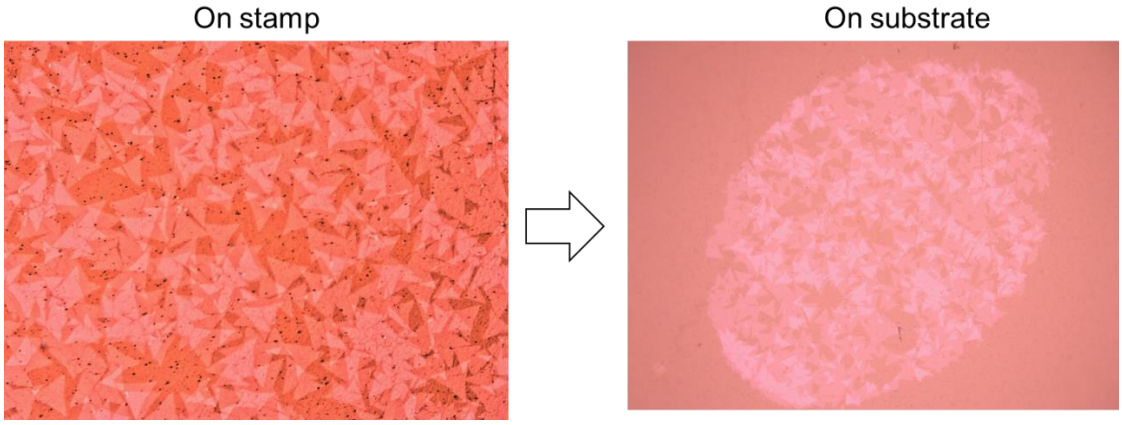

Figure S12. The pick-up of WS2 and that dropped off on to substrate.

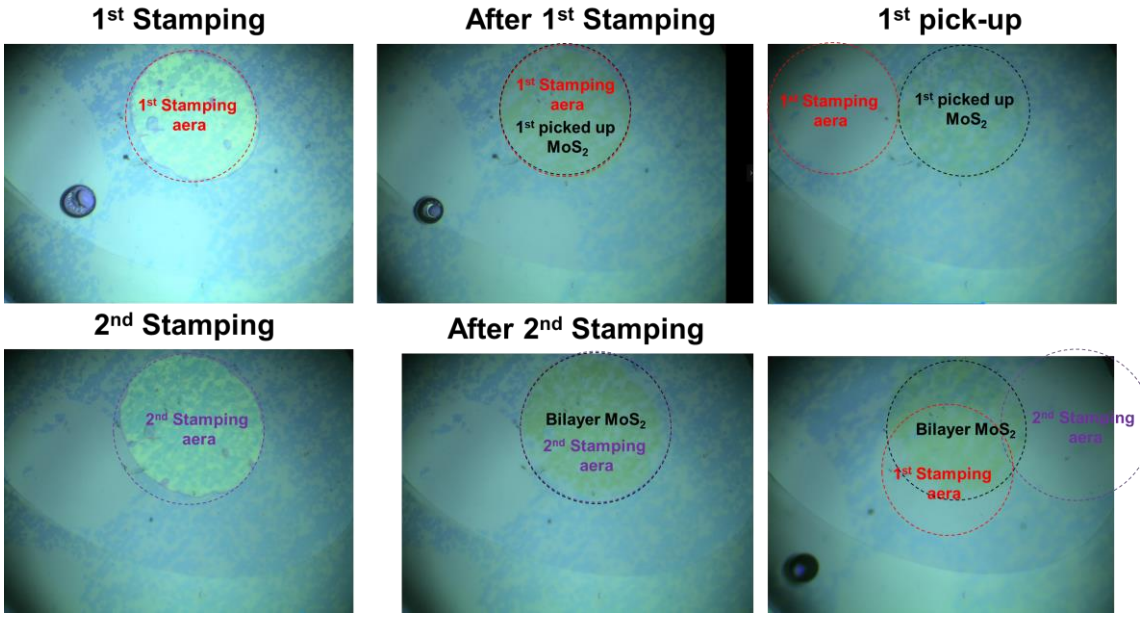

Figure S13. screenshot of the process stacking of MoS_2 in SI movie.

Stamp / Polymer	a. PMMA			b. PDMS/DMSO (Dimethyl sulfoxide)	c. PDMS (Dimethylpolysiloxane)	d. PDMS/PVA (polyvinyl alcohol)	e. Polystyrene (PS)
Methology	PMMA direct spin coating on targeted 2D flaks			Transfer with solid PDMS/DMSO stamp	Transfer with solid PDMS stamp	Transfer with solid PDMS/DMSO stamp	PS direct spin coating on substrate
Pick-up	Etching (NaOH/KOH)	Bubbling transfer (NaCl solution)	Desolve the water-soluble sacrificial layer	Heating at 70 ◦C	Dry+water@70 ℃	Dry pickup	Wet+ water
Drop-off	PMMA removed by chemical method			Dry release	Dry release	Wet release (PVA remove by water)	Wet (PS removed by THF)
Sequential pick-up	X	X	X	X	X	X	X
large scale transfer	O	O	O	O	O	O	O
Spatial resolved micro-scale transfer	X	X	X	O	O	O	X
Other advantages & disadvantages	✓ The adhesion between substrate and 2D flaks do not influence pick-up X Substrate not reusable X 2D flakes on SiO_2/Si substrate only X Additional annealing in Ar/H2 to remove PMMA	✓ The adhesion between substrate and 2D flaks do not influence pick-up X For metal substrate only	✓ The adhesion between substrate and 2D flaks do not influence pick-up X Substrate not reusable X 2D flakes on water soluable substrate only (NaS_x and NaCl)	✓ Less polymer residual ✓ All dry process (fast)	✓ All dry process (fast) X For MoS2 on SiO2 substrate only	✓ PVA is water-solubility (less residual) ✓ good adhesion to 2D flaks (high versatile) X Hard for uniform transfer	✓ Large young' modulus -> less deformation of 2D flaks X Weak adhesion between PS and 2D flaks
Targeted 2D materials	MoS2 (on etchable substrate)	WS2	MoS2	MoS2	MoS2 on SiO2/Si substrate	WSe2	MoS2 on sapphire
Ref.	Nanoscale 4 6637(2021) Appl. Phys. Lett. 104 203506 (2014)	ACS Nano 9 5510 (2015) ACS Nano 5 9927 (2011)	Nanoscale 9 19124 (2017)	Carbon 116 167 (2017)	Nanoscale 8 10677 (2016)	IEEE Access 8 70488 (2020)	ACS Nano 8 11522 (2014)

f. PS	g. CA (Cellulose acetate)	i. PET/EVA (Ethylen-Vinyl Acetate)	j. PVA/PVP (Polyvinylpyrrolidone)	k. TRT tape/PMMA	This study: P-PVC
PS direct spin coating on substrate	CA direct spin coating on substrate	Transfer with solid EVA/PET stamp	Transfer with solid PVA/PVP stamp	Use TRT/PMMA/2D flake as stamp	Use P-PVC/PDMS as stamp
Wet + NaOH	Wet + NaOH or NH4F and HF	Dry + water	Dry	Dry	Dry + water @70ºC
wet	Wet (CA removed by aceton)	- (no drop off)	Wet (PVP is water soluble)	PMMA should be removed by heating or chemical solution	Wet (PVC removed by THF+annealing)
X	X	X	X	O	O
X	O	O	O	O	O
X	X	△	△	X	O
✓ damage to the sapphire substrate ✓ PS is brittle(not suitable for large aera)	✓ Less residual, and wrikles	✓ Large scale, all dry process ✓ Enables Roll to roll transfer	✓ Good adhesion X Need to tune the contact of PVP and 2d flaks with extra chemical (N-vinylpyrrolidone)	✓ Clean interface ✓ Large aera X spin coating process (1st layer)	✓ Fast assembling of vdWs hetrostructure ✓ For both micro and macro scale fabrication
MoS2, WS2	TMD on SiO2	MoS2	MoS2, WS2	MoS2, WS2, MoSe2…	MoS2, WS2,
ACS Nano 9 6178 (2015)	ACS Appl. Nano Mater. 2 5320 (2019)	Nat. Commun. 9 979 (2018)	ACS Nano 10 5237 (2016)	Nature 550 229 (2017)	

Table S1. comparison of transfer method for CVD-grown 2D flakes[4,5,14,6–13]

Reference

1. Wakafuji, Y. *et al.* Evaluation of polyvinyl chloride adhesion to 2D crystal flakes. *npj 2D Mater. Appl.* **6**, 4–6 (2022).
2. Wakafuji, Y. *et al.* 3D Manipulation of 2D Materials Using Microdome Polymer. *Nano Lett.* **20**, 2486–2492 (2020).
3. Sood, A. *et al.* Engineering Thermal Transport across Layered Graphene-MoS2Superlattices. *ACS Nano* **15**, 19503–19512 (2021).
4. Lin, Y.-C. *et al.* Wafer-scale MoS2 thin layers prepared by MoO3 sulfurization. *Nanoscale* **4**, 6637 (2012).
5. Amani, M. *et al.* Growth-substrate induced performance degradation in chemically synthesized monolayer MoS2 field effect transistors. *Appl. Phys. Lett.* **104**, 203506 (2014).
6. Zhang, L. *et al.* Damage-free and rapid transfer of CVD-grown two-dimensional transition metal dichalcogenides by dissolving sacrificial water-soluble layers. *Nanoscale* **9**, 19124–19130 (2017).
7. Yang, P. *et al.* Batch production of 6-inch uniform monolayer molybdenum disulfide catalyzed by sodium in glass. *Nat. Commun.* **9**, 1–10 (2018).
8. Cao, Y. *et al.* Movable-Type Transfer and Stacking of van der Waals Heterostructures for Spintronics. *IEEE Access* **8**, 70488–70495 (2020).
9. Yun, S. J. *et al.* Synthesis of centimeter-scale monolayer tungsten disulfide film on gold foils. *ACS Nano* **9**, 5510–5519 (2015).
10. Lin, Y. C. *et al.* Clean transfer of graphene for isolation and suspension. *ACS Nano* **5**, 2362–2368 (2011).
11. Shim, G. W. *et al.* Large-area single-layer MoSe2 and its van der Waals heterostructures. *ACS Nano* **8**, 6655–6662 (2014).
12. Kang, K. *et al.* Layer-by-layer assembly of two-dimensional materials into wafer-scale heterostructures. *Nature* **550**, 229–233 (2017).
13. Xu, Z. Q., Xia, X. & Bao, Q. Synthesis and Transfer of Large-Area Monolayer WS2 Crystals: Toward the Recyclable Use of Sapphire Substrates. *Opt. InfoBase Conf. Pap.* 6178–6187 (2015) doi:10.1364/soled.2015.dtu3d.2.
14. Gurarslan, A. *et al.* Surface-energy-assisted perfect transfer of centimeter-scale monolayer and few-layer MoS2 films onto arbitrary substrates. *ACS Nano* **8**, 11522–11528 (2014).